Development of Hollow Cathodes for 5 to 20 kW Hall Thrusters

IEPC-2017-364

Presented at the 35th International Electric Propulsion Conference
Georgia Institute of Technology • Atlanta, Georgia • USA
October 8 – 12, 2017

Daniela Pedrini[1] and Federico Torrini[2]
SITAEL, Ospedaletto, Pisa, 56121, Italy

Jacopo Grassi[3] and Fabrizio Paganucci[4]
University of Pisa, Pisa, 56126, Italy

and

Tommaso Andreussi[5], Tommaso Misuri[6] and Mariano Andrenucci[7]
SITAEL, Ospedaletto, Pisa, 56121, Italy

Abstract: The use of electric propulsion systems is growing wider for military and commercial applications, as well as scientific missions. The benefits provided by electric propulsion are tied to a lower propellant mass with respect to chemical propulsion, allowing for a higher payload mass, a lower total mass, therefore less expensive launch vehicles. Hall effect thrusters provide an optimal trade-off between specific impulse and thrust, along with a lower power-to-thrust ratio with respect to other electric propulsion technologies. For the high-power class of thrusters, the cathodes must be able to sustain operating currents up to several tens of amperes. In this context, two lanthanum hexaboride (LaB_6) hollow cathodes have been developed and tested at Sitael, conceived for Hall thrusters in the range 5 – 20 kW. The cathodes for 5 kW-class Hall thrusters, HC20 and HC20h, are required to provide discharge currents in the 8 – 20 A range, with a lifetime in excess of 10^4 hours. The hollow cathode to be coupled with 20 kW-class Hall thrusters operates at discharge currents up to 60 A, hence the name HC60. The cathodes were characterized during stand-alone test campaigns, as well as with the respective Hall thrusters. The experimental results will be presented and compared with the predictions from a previously developed model describing the operation of thermionic hollow cathodes, showing a good agreement between empirical and theoretical data. The model was expanded to consider the cathode plume exiting from the keeper. As a matter of fact, a two-fluid description of the plasma between the keeper and an anode plate was implemented in a numerical model, which will be described and whose results will be discussed and compared with the available experimental data.

[1] Electric Propulsion Design Engineer, PhD, Space Propulsion Business Unit, daniela.pedrini@sitael.com
[2] Project Scientist, Space Propulsion Business Unit, federico.torrini@sitael.com
[3] Graduate Student, Department of Civil and Industrial Engineering, jac92gr@yahoo.it
[4] Associate Professor, Department of Civil and Industrial Engineering, f.paganucci@ing.unipi.it
[5] EP Technology Development Engineer, PhD, Space Propulsion Business Unit, tommaso.andreussi@sitael.com
[6] Head, Space Propulsion Division, tommaso.misuri@sitael.com
[7] Head, Space Propulsion Division, mariano.andrenucci@sitael.com

Nomenclature

m_i	=	ion mass
m_e	=	electron mass
S	=	ionization rate
v_{j-i}	=	collision frequency between the species j and i
K_b	=	Boltzmann constant
U_{ion}	=	ionization energy of neutrals
γ_n	=	adiabatic coefficient for neutrals
γ_i	=	adiabatic coefficient for ions
n_n	=	neutral density
u_n	=	neutral fluid velocity
T_n	=	neutral temperature
n_i	=	ion density
u_i	=	ion fluid velocity
T_i	=	ion temperature
n_e	=	electron density
u_e	=	electron fluid velocity
T_e	=	electron temperature
n	=	plasma density
ϑ	=	neutral expansion angle

I. Introduction

THE use of high-power electric thrusters is increasingly fostered for a number of different maneuvers, including final positioning and station-keeping of Geostationary Earth Orbit (GEO) satellites, spacecraft transfers from Geostationary Transfer Orbit (GTO) to GEO, or from Low Earth Orbit (LEO) to other high-altitude orbits, and deep-space missions, as demonstrated by Deep Space 1, SMART-1, Hayabusa, and Dawn[1-4]. Hall Effect Thrusters (HETs) provide an optimal trade-off between specific impulse and thrust, along with a lower power-to-thrust ratio with respect to other electric propulsion technologies. These peculiarities promote the use of Hall thrusters for both military and commercial applications, as well as scientific missions. The development of high power (>10 kW) Hall thrusters also represents an important step to improve the propulsion systems capabilities for space exploration, allowing for acceptable missions durations.

Sitael is active in this field, through the development of 5 kW- and 20 kW-class Hall effect thrusters, for which the cathodes must be able to sustain operating currents up to several tens of amperes[5]. HT5k operates in the 2.5 – 7.5 kW range to produce a thrust comprised between 150 and 350 mN and a specific impulse in the 1700 – 2800 s range[6]. A magnetically shielded version of HT5k was also developed, referred to as HT5k LL, as described in Ref. 7. HT20k is a thruster designed to operate at a nominal discharge power of 20 kW to produce a thrust greater than 1 N and a specific impulse higher than 2500 s[8]. Two hollow cathodes were developed for the 5 kW-class Hall thrusters, namely HC20 and HC20h, whereas HC60 is the cathode conceived for HT20k. The cathodes were successfully operated with xenon and krypton. The interest in krypton is tied to the reduction of on-ground development and qualification costs, and also to relax the dependence on the volatile natural-resource market[9].

II. Cathode Design

The general architecture adopted for the cathode design is schematically shown in Fig. 1. An orificed thin tube, made of a refractory metal (e.g. tantalum or molybdenum alloy), is fed with the propellant, usually xenon or krypton. The emitter or insert is placed inside the tube, in contact with the orifice by means of a spring-spacer system. The emitter is a hollow cylinder made of lanthanum hexaboride (LaB_6), which provides electrons through the field-enhanced thermionic effect. The boride compound has been selected for its low evaporation rate and low sensitivity to contaminants and air exposure, despite the higher work function with respect to traditional dispenser cathodes (based on barium oxide compounds). As a matter of fact, the work function of polycrystalline LaB_6 is comprised in the range 2.4 – 2.7 eV[10,11], whereas a barium-based emitter has a work function of about 2.1 eV[12]. Consequently, the operating temperature of a LaB_6 emitter to provide a current density in the order of 10^5 A/m^2 is about 1900 K, as compared to about 1300 K for dispenser emitters.

An electrode called keeper is used to initiate the discharge through the application of a positive potential with respect to the main tube. Additional functions of the keeper are to help the emitter in maintaining its operating surface temperature, and to protect the internal parts from ion bombardment. As soon as the discharge is established, the heater is turned off and the cathode operates in a self-heating mode. A heater was included in the assembly of both HC20h and HC60 to ease the cathode ignition, by heating the emitter up to thermionic emission values. The heater consists of a refractory metal filament, wrapped around the cathode tube from which is electrically insulated by means of ceramic parts. The heater is surrounded by heat shields, used to limit the power loss towards the keeper, thus improving the thermal behavior of the cathode. HC20h and HC60 are shown in Fig. 2, before the respective characterization campaigns.

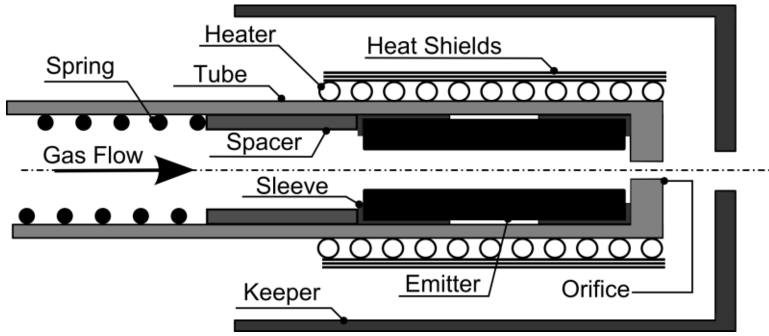

Figure 1. General schematic of an orificed hollow cathode.

The main functional dimensions of the cathode derive from a theoretical model developed at Sitael to describe the operation of orificed hollow cathodes, whose results were analyzed to select the emitter inner and outer diameters, the emitter length, and the orifice diameter and length. The cathode model is a volume-averaged model which considers the plasma created inside the cathode as divided in three regions encompassing the emitter, the orifice, and the cathode-to-keeper gap[13,14]. Systems of particle and energy balance equations in steady-state conditions are self-consistently solved for a given cathode geometry and operating point (namely, discharge current and mass flow rate).

A dedicated lumped-parameter thermal model is coupled with the plasma model, and the combined systems of equations are solved by means of an iterative procedure to compute the plasma parameters, temperature profile, and total discharge power. The pressure model is based on a Poiseuille flow in the orifice region[15], with a correction term for the transitional regime as a function of the Knudsen number. Since the electron temperature in a hollow cathode plasma is low (1 – 3 eV) in comparison to the first ionization energy of the neutrals (about 12 eV for xenon, about 14 eV for krypton), the stepwise ionization process will dominate over the direct-impact mechanism. As such, the ionization model includes the contribution of the step-wise mechanism[16].

The cathode lifetime is evaluated according to the evaporation rate of the emitter at the computed surface temperature[13], even though other mechanisms such as orifice clogging and ion bombardment damage could cause a performance degradation shortening the cathode lifetime. In parallel with the theoretical study, the possible alternatives of materials for the different cathode parts were evaluated, to select the best combination for improving the thermal behavior of the cathode, as verified by the cathode model. The model was validated against experimental data of cathodes belonging to different power classes[13,14]. A further theoretical study was performed, by developing a model of the cathode plume exiting from the keeper, as described in the following section.

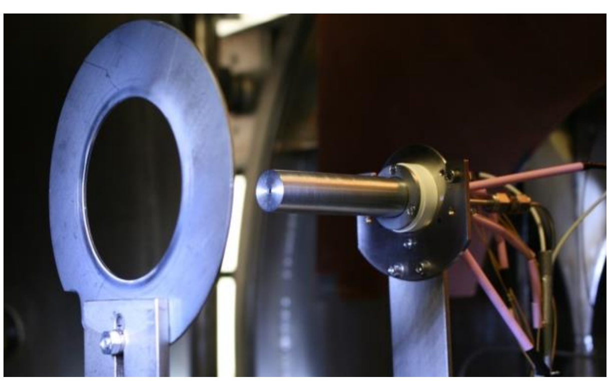

a)

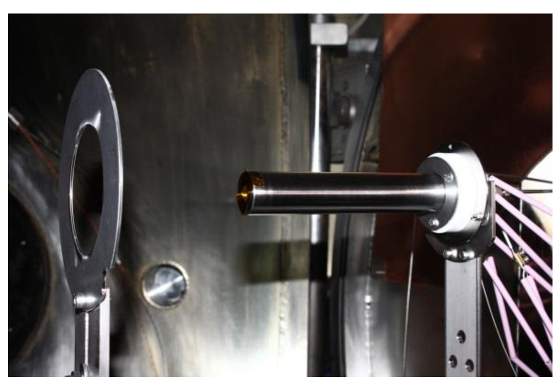

b)

Figure 2. Setup of the cathodes for the stand-alone test campaigns: a) HC20h. b) HC60.

III. Theoretical Model of the Cathode Plasma Plume

A. Plume Model Description

The plume model was conceived as a logical extension of the pre-existent model of the cathode internal regions, with the purpose of describing the parameters of the cathode plume. The importance of understanding the phenomena outside the cathode arises from various important reasons:

- understanding the presence of high energy ions and limit the keeper erosion;
- studying and cutting out the plasma instabilities;
- improving the cathode electrical characteristics and the cathode-thruster coupling.

It is well-known (see e.g. Ref. 12) that the plume region plasma is collisionless (the plasma frequency, ω_p, is higher than the collisions frequencies, υ_{col}: $\omega_p > \upsilon_{col}$), making this region unsuitable to be described with a fluid model. In addition, the 1-D description is not able to properly characterize the 2-D nature of the flow. Nevertheless, the 1-D fluid model has proved to be useful, since it captures the main physical phenomena of the plume region.

The general setup considered in the model is a hollow cathode with an external anode plate collecting the current and located at a fixed distance from the keeper exit section. The model consists of a system of ten differential equations: the continuity equation, the equation of motion, the energy equation for each of the three species (electrons, ions, and neutrals), and an equation describing the expansion angle of the neutrals. The presence of fluid instabilities in the plume region implies flow turbulence and an anomalous potential grow, which are accounted for by means of a free parameter: the resistivity coefficient, C_r.

Given the different properties of each species and the typical plasma parameters of the cathode plume, each fluid is treated differently. In the electron equation of motion, the inertial term is neglected[17], and both the density and the temperature gradients are considered, requiring the inclusion of an electron energy equation. On the contrary, the inertia term is considered for both ions and neutrals, and the energy equation is replaced by the usual density-temperature relation in which an adiabatic coefficient is assumed[17]. The momentum exchange due to collisions between all the species is considered. The last differential equation describes the expansion angle of the neutral flow, according to the neutral thermal velocity. Given the presence of anomalous transport phenomena[17], the fluid model is not able to properly evaluate the electron temperature and, in turn, the Bohm velocity which affects the plasma expansion angle. As such, the plasma expansion angle is assumed to be constant.

Quasi-neutrality is assumed throughout all the computation domain, namely the ion density, n_i, is set equal to the electron density, n_e: $n_i = n_e = n$. The ten equations allow for computing the ten unknowns of the problem: neutral density, n_n, neutral fluid velocity, u_n, neutral temperature, T_n, plasma density, n, ion fluid velocity, u_i, ion temperature, T_i, electron fluid velocity, u_e, electron temperature, T_e, electric field, E, and neutral expansion angle, ϑ. The equations are summarized in the following, with the exception of the one describing the neutral expansion angle, which is reported in detail in Ref. 18:

Neutral Continuity Equation

$$\nabla \cdot (u_n n_n) = -S \tag{1}$$

Neutral Equation of Motion

$$m_i \nabla (n_n u_n^2) = -\gamma_n K_b T_n \nabla n_n - m_e n C_r \upsilon_{e-n}(u_n - u_e) - 2 m_i n C_r \upsilon_{i-n}(u_n - u_i) \tag{2}$$

Neutral Energy Equation

$$\frac{\nabla T_n}{T_n} = (\gamma_n - 1)\frac{\nabla n_n}{n_n} \tag{3}$$

Ion Continuity Equation

$$\nabla \cdot (u_i n) = S \tag{4}$$

Ion Equation of Motion

$$m_i \nabla(n u_i^2) = qnE - \gamma_i K_b T_i \nabla n - m_e n C_r \upsilon_{e-i}(u_i - u_e) + 2 m_i n C_r \upsilon_{i-n}(u_n - u_i) \tag{5}$$

Ion Energy Equation

$$\frac{\nabla T_i}{T_i} = (\gamma_i - 1)\frac{\nabla n}{n} \tag{6}$$

Electron Continuity Equation

$$\nabla \cdot (u_e n) = S \tag{7}$$

Electron Equation of Motion

$$0 = -qnE - \nabla K_b T_e n + m_e n C_r \upsilon_{e-n}(u_n - u_e) + m_e n C_r \upsilon_{i-n}(u_n - u_i) \tag{8}$$

Electron Energy Equation

$$\nabla \cdot \left[\left(\frac{1}{2} m_e u_e^2 + \frac{5}{2} K_b T_e\right) n u_e\right] = -qnE \cdot u_e - \frac{1}{2} m_e n C_r \upsilon_{e-i}(u_i - u_e)^2 - \frac{1}{2} m_e n C_r \upsilon_{e-n}(u_n - u_e)^2 - S U_{ion} \tag{9}$$

where m_i is the ion mass (taken equal to the neutral mass), m_e the electron mass, S the ionization rate, υ_{j-i} the collision frequency between the species j and i, K_b the Boltzmann constant, U_{ion} the ionization energy of neutrals, γ_n and γ_i the adiabatic coefficient for neutrals and ions, respectively.

B. Comparison with Experimental Data

A preliminary validation of the model for the cathode plasma plume has been carried out, comparing the theoretical results with data available in the literature, namely referring to the following hollow cathodes: NEXIS[19], NSTAR[20], and a hollow cathode from JAXA[21]. Representative comparisons are shown in Fig. 3, in terms of plasma potential and plasma density as a function of the distance from the keeper exit section, for the NEXIS cathode operated at 25 A and 0.55 mg/s Xe. The comparison highlighted that the model results are in good accordance with the experimental data (excluding the electron temperature). The free parameter, C_r, has been set equal to 15, allowing for predicting a total potential difference from the keeper orifice to the anode within an error of 10% from experimental data. Nevertheless, the model is not able to predict the correct trend of the plasma potential as a function of the axial distance, due to the aforementioned instabilities. The model results suggested the presence of a current instability[22] (due to the high electron drift velocity), whose effects on the potential difference and the electron temperature will be included in the future development of the model. In addition, the plume model will be coupled with the model of the cathode internal regions previously developed at Sitael[13,14], to obtain a more complete description of the physical phenomena occurring in the cathode when operated with an auxiliary anode plate.

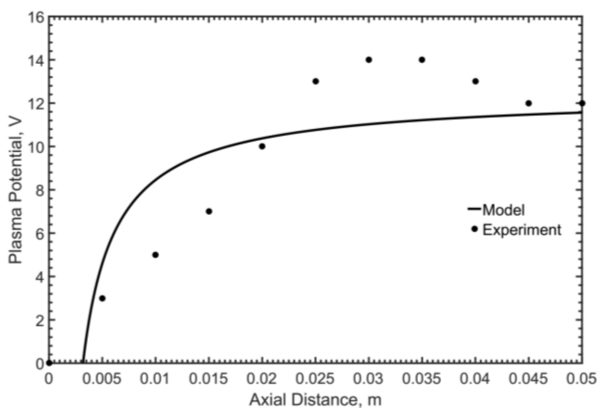

a)

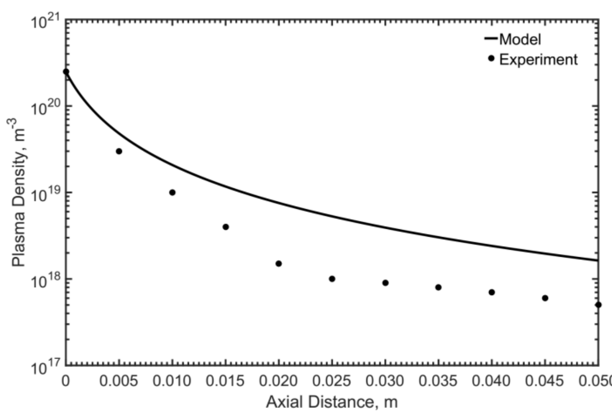

b)

Figure 3. Comparison of theoretical and experimental results for the NEXIS cathode[19]: plasma potential (a) and plasma density (b) as a function of the axial distance, at 25 A and 0.55 mg/s Xe.

IV. Experimental Setup

The cathodes were tested at Sitael in vacuum chambers of different size. The experimental campaigns included both stand-alone characterization and coupling tests with the respective Hall thrusters.

A. LFF Vacuum Chamber

LFF consists of two stainless steel AISI 316 vessels: the main chamber (MC) and the auxiliary chamber (AC). The main chamber has a diameter of 1.2 m and a length of 2.8 m, whereas the auxiliary chamber is a 0.5 m-diameter, 1 m-length service chamber. The two volumes are connected by a large gate valve (LGV) which can be exploited to use the auxiliary chamber as recovery area during maintenance and regeneration of the MC. LFF is equipped with two separated pumping systems. The main pumping system (MPS) is located in the MC and includes a rotary pump Varian Triscroll PTS 600 (28 m^3/h) for fore vacuum, a turbopump Varian TV-2000HT (2000 l/s) for high vacuum, a cryopump Leybold Coolvac 1500 for ultra-high vacuum, and a cold head Leybold Coolpower 140T. The auxiliary pumping system (APS), located in the AC, includes a rotary pump Varian Triscroll PTS 300 (15 m^3/h) for fore vacuum and a turbopump Varian V-301HT (300 l/s) for high vacuum. The pressure level in the chamber is continuously monitored by one sensor Alcatel AHC 1010 and one sensor Leybold ITR90 both placed in the AC, and two sensors Leybold ITR90 placed in the MC. The facility can reach an ultimate pressure lower than 5×10^{-6} Pa. LFF is shown in Fig. 4.

Figure 4. LFF facility.

B. IV4 Vacuum Chamber

The IV4 facility consists of two different bodies made of AISI 316L stainless steel with low magnetic relative permeability (μ_r<1.06). The main chamber has a diameter of 2 m and a length of 3.2 m, whereas the small chamber is a 1 m-diameter, 1 m-length service chamber. The two bodies are connected through a 1 m-diameter gate valve. The small chamber was used to accommodate the cathode setup, its electrical and gas-feeding systems, whereas the main chamber allowed for a free expansion of the plasma plume and it is directly connected to the main pumping system. A bi-conical, water cooled, Grafoil-lined target is installed in order to dump the beam energy down. The chamber pumping system is capable of maintaining a back pressure in the range of 10^{-5} Pa (ultimate vacuum) by using a primary stage located in the main chamber and a secondary stage located in the small chamber. The combined pumping speed of the system is approximately 1.3×10^5 l/s for xenon. The pressure level within the chamber is continuously monitored by three Leybold-Inficom IT90 Pirani/Bayard-Alpert sensors and recorded via

a)

b)

Figure 5. a) IV4 facility. b) IV10 facility.

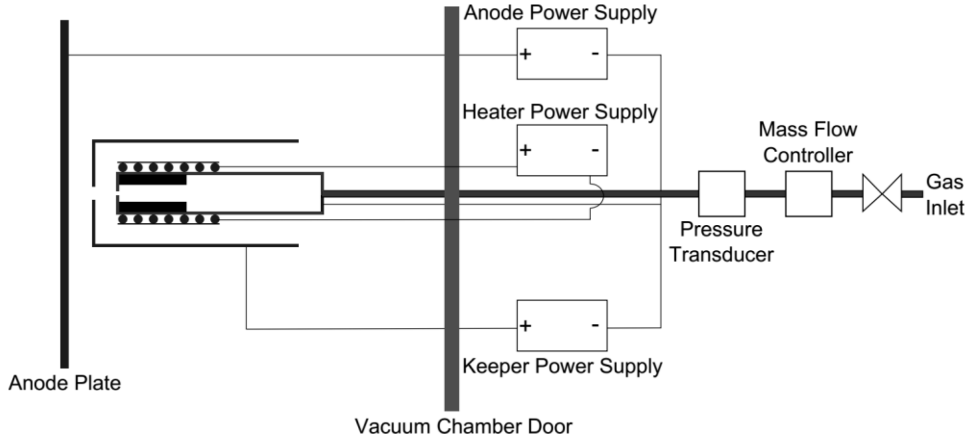

Figure 6. General test schematic for the cathode characterization.

LabVIEW. IV4 is the facility where the coupling tests of cathode and thruster were performed. The IV4 vacuum chamber is shown in Fig. 5a.

C. IV10 Vacuum Chamber

The IV10 vacuum chamber is made of a cylindrical stainless steel body 5.74 m in diameter and 9.40 m in length. The facility is equipped with two 2000 l/s turbo molecular pumps, two scroll pumps, two 5000 l/s cryogenic pumps, and five 60000 l/s cold panels. The ultimate vacuum in the chamber is as low as 3×10^{-7} Pa. The IV10 vacuum chamber is shown in Fig. 5b.

D. General Test Schematic

The general test schematic adopted for the cathodes characterization is shown in Fig. 6. A current-limited Huttinger PFG5000 (1000 V, 6 A) power supply controlled the cathode-to-keeper voltage during discharge initiation and the keeper current during operation for HC20, whereas the same functions were performed by a Magna Power TSD 1000-15 (1000 V, 15 A, 15 kW) power supply for HC60. The cathode to-anode current was controlled using a Sorensen DLM 150-20E (150 V, 20 A) power supply for HC20 and HC20h, whereas a Regatron TopCon TC.P.20.500.400.S (500 V, 50 A, 20 kW) was used to supply the anode current to HC60. A TTI CPX400DP (dual isolated outputs, 60 V, 20 A) power supply was used to control both the keeper and the heater of HC20h, whereas the heater of HC60 was controlled using a Sorensen DLM 300-3.5E (300 V, 3.5 A) power supply. All the power supplies were connected to a common negative reference and the setup was electrically floating with respect to ground. The electrical parameters were measured by using current (LEM LA25-NP) and voltage (LEM LV25-P) probes, with the exception of the current probe measuring the anode current of HC60, selected as LEM LA55-NP. All the sensing probes were calibrated before the test and connected to the DAQ system controlled via LabVIEW software. The error associated with the DC voltage measurements is ±2%, whereas a relative error of ±1% is evaluated for the current measurements. The cathode gas feeding line was equipped with a dedicated mass flow controller (Bronkhorst F-201C-FAC-22-V), connecting the xenon tank to the test item. High purity (grade N48) xenon and krypton were used during the test campaigns. The pressure in the cathode line was monitored by means of a pressure transducer, namely MKS 722A13MGA2FA, whose accuracy is 0.5% of the measured values and whose full scale range is 1000 torr. K-type thermocouples were installed on the mounting flange constituting the mechanical interface, on the outer keeper flange, and on the backside of the anode, to monitor the integrity of the materials during extended operation.

V. HC20 and HC20h: 8 to 20 A Hollow Cathodes

Two cathodes for 5 kW Hall effect thrusters have been developed and tested at Sitael: HC20 is a heaterless cathode whose description is detailed in Ref. 23, whereas HC20h is a new version of the previous cathode. The main differences between the two cathodes lie in the inclusion of a heater and in the emitter dimensions. As a matter of fact, HC20h includes a heater, whereas HC20 was conceived as a heaterless cathode. In addition, HC20h is a more compact cathode, whose main dimensions were selected on the basis of the in-house model after the implementation of a number of modifications and improvements[5]. Both the cathodes were conceived for the 8 – 20 A range (1 – 4 mg/s mass flow rate), with an expected lifetime higher than 10^4 hours. The cathode mass (without cables) is about 350 grams for HC20, and about 160 grams for HC20h.

The ignition procedure of HC20h consisted in a heating phase, during which a power of about 100 W was supplied to the heater, which allowed for starting the discharge with a keeper voltage as low as about 25 – 40 V, with a mass flow rate of 1 mg/s Xe. The ignition procedure was substantially different with respect to HC20, which required 800 V applied to the keeper and 130 V applied to the anode, at 5 mg/s Xe, without any pre-heating phase[23].

HC20 performed a new characterization test campaign, including measurements of the anode voltage oscillations, at current levels up to 20 A, with an external anode plate located 65 mm downstream of the keeper exit section. The experiments showed a successful operation of the cathode in the selected range of operating conditions. Fig. 7a shows the voltage-flow rate characteristics of HC20 operated in triode mode, at different anode currents and with 2 A keeper current. The sudden increase in keeper voltage at low mass flow rates indicates the onset of plume-mode, as suggested by similar trends found in the literature[15].

The anode voltage oscillations were measured by an oscilloscope and are reported in Fig. 7b in terms of the peak-to-peak anode voltage as a function of the mass flow rate, during operation with a keeper current of 2 A. According to the Brophy criterion for identifying the plume mode operation[24], the cathode enters the plume mode region when the mass flow rate is decreased below 1.5 mg/s, except for the lowest value of the anode current tested (i.e. 2 A), at which the cathode remains in spot mode down to 1 mg/s. With the keeper left floating, the cathode operated in spot mode at mass flow rates higher than 2.5 mg/s, below which the cathode transitioned to the plume mode. The theoretical model was used to compute the electrical characteristics of HC20: representative results are reported in Fig. 8 for xenon and krypton[23], showing a good agreement with the experimental data.

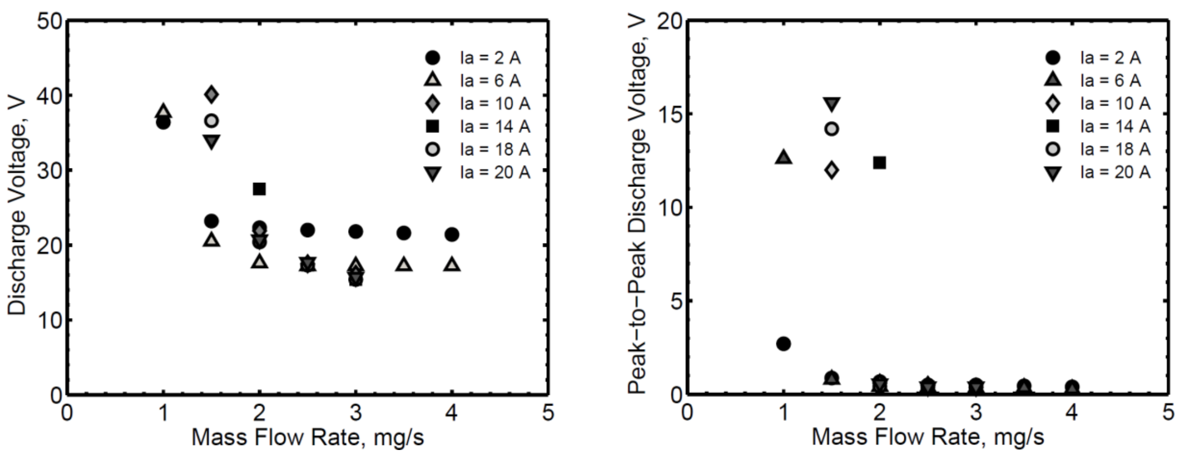

a) **b)**

Figure 7. Discharge voltage (a) and peak-to-peak discharge voltage (b) as a function of mass flow rate, at different anode currents and 2 A keeper current.

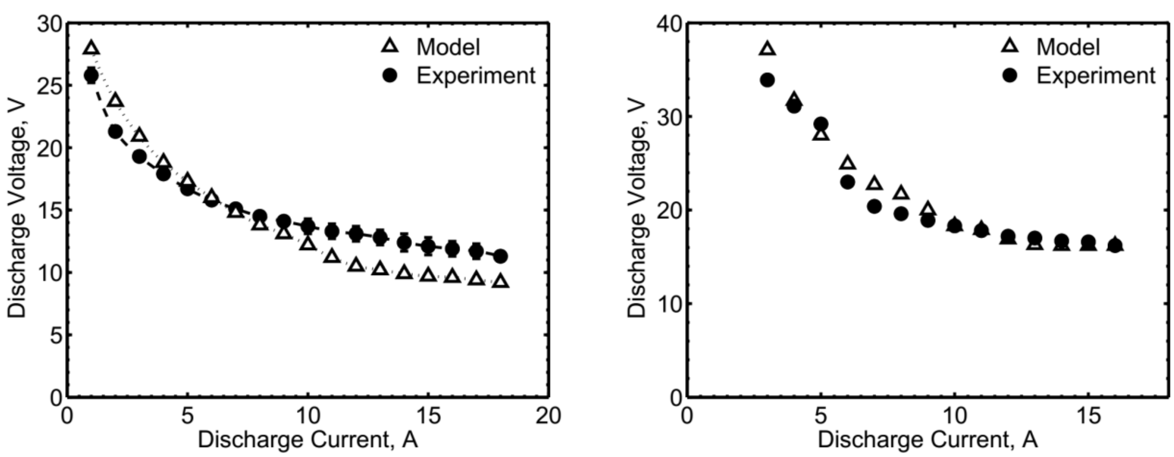

a) **b)**

Figure 8. Comparison between experimental and theoretical characteristics, in triode mode at 1 mg/s and 2 A keeper current, with xenon (a) and krypton (b).

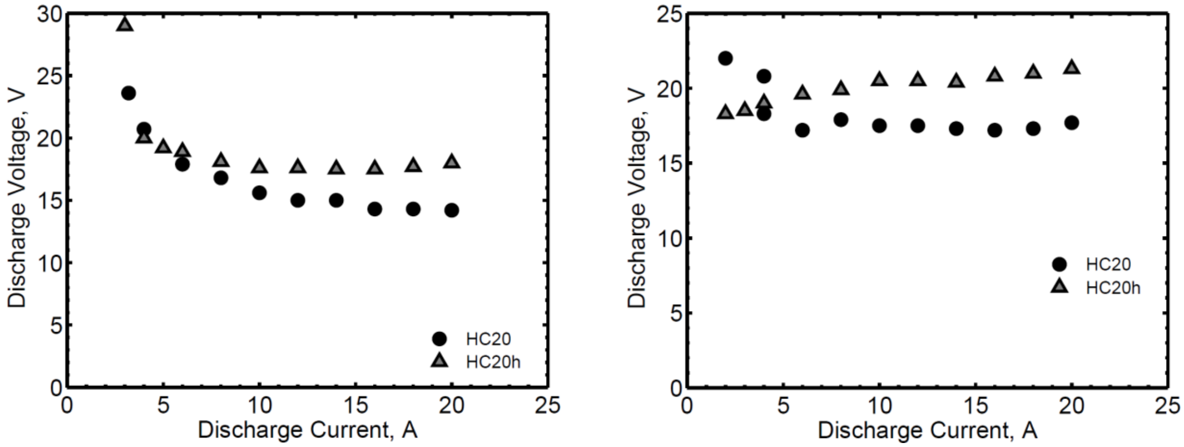

a) b)

Figure 9. Comparison of electrical characteristics of HC20 and HC20h at 4 mg/s and floating keeper (a), and at 2.5 mg/s with 2 A keeper current (b).

HC20h was tested in a similar configuration with respect to HC20, maintaining the same anode distance from the keeper. Representative comparisons of the experimental electrical characteristics of the two cathodes are reported in Fig. 9a for the operation with floating keeper at 4 mg/s Xe, and in Fig. 9b with 2 A keeper current and 2.5 mg/s Xe. According to Fig. 9a, the electrical characteristics follow the typical trends as found in the literature, although the discharge power of HC20 was up to 23% lower with respect to HC20h. Also the operation with the keeper showed a discharge power up to about 19% lower for HC20 with respect to HC20h (Fig. 9b). These trends suggest that HC20h has an operating envelope shifted towards lower currents as compared to HC20, still being able to sustain the discharge of a 5 kW-class Hall effect thruster.

HC20h is shown in Fig. 10 during the stand-alone test campaign and coupled with the Sitael magnetically shielded 5 kW thruster, in center-mounted position. HC20 operated for about 350 hours and was ignited about 140 times during the latter test campaigns (both in stand-alone configuration and coupled with HT5k LL), adding up to 1000 hours of operation and more than 350 ignitions previously performed[23]. HC20h in total cumulated about 100 hours and more than 160 ignitions.

VI. HC60: 30 to 60 A Hollow Cathode

HC60 was conceived to operate at mass flow rates between 2 and 6 mg/s, at discharge currents between 30 and 60 A. The cathode predicted lifetime should be higher than 10^4 hours, whereas the cathode mass without cables is about 450 grams.

The cathode was initially tested in a stand-alone setup, to perform a characterization campaign before being coupled with the Sitael HT20k thruster[8]. During the dedicated tests in a stand-alone configuration, HC60 was characterized with both xenon and krypton propellants. A satisfactory operation of the cathode was observed with

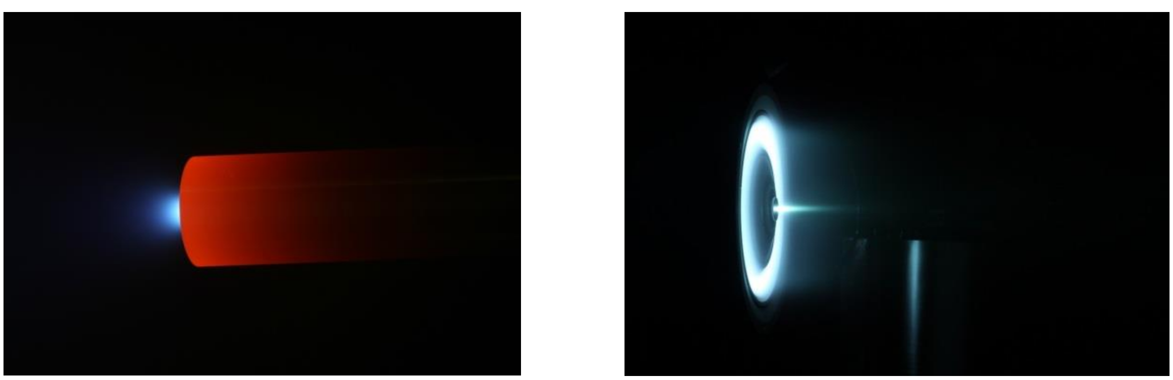

a) b)

Figure 10. a) HC20h operating in xenon with the anode at 20 A and floating keeper. b) HC20h during a coupling test with Sitael HT5k LL[7].

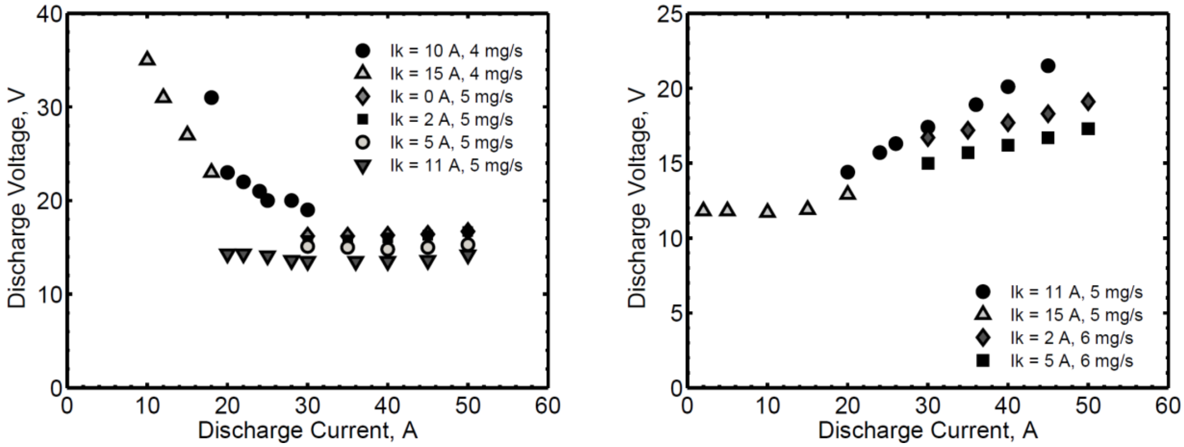

a) **b)**

Figure 11. Electrical characteristics at different keeper currents and mass flow rates, with xenon (a) and krypton (b).

both propellants in the investigated range of operating conditions. After the characterization tests, HC60 was coupled with the HT20k thruster, both externally and in a center-mounted configuration.

The cathode was ignited with the aid of a heater, whose power level of about 165 W allowed for starting the cathode by flowing 5 mg/s Xe and applying a voltage lower than 500 V at the keeper. Heaterless ignitions were performed as well, at the cost of higher keeper voltage and mass flow rate, namely about 900 V and 12 mg/s Xe, respectively. Similar ignition parameters were used to start the cathode with krypton propellant.

During the cathode stand-alone test campaign, an external anode plate was located 100 mm downstream of the keeper orifice section. HC60 was firstly operated with the keeper only, between 11 and 15 A, at mass flow rates in the range 3 – 5 mg/s, with xenon and krypton. The cathode was then tested in triode mode with xenon, at a total current up to 60 A (50 A anode current, 10 A keeper current). A cathode pressure in the range 40 – 56 hPa was measured, increasing with both the discharge current and the mass flow rate (3 – 5 mg/s Xe). The cathode pressure during operation with krypton ranged from about 68 to 82 hPa, at mass flow rates between 5 and 6 mg/s. The operation with krypton required a mass flow rate of at least 5 mg/s to run the cathode in triode mode with the anode. At 6 mg/s Kr, the lowest keeper current which allowed for sustaining a discharge of 30 – 50 A at the anode was 2 A. As a matter of fact, the cathode was not able to operate in diode mode with the anode with krypton, whereas an anode current of 50 A with keeper off was sustained with xenon, at 4 mg/s. The results of the characterization are reported in Fig. 11 for both xenon and krypton. During operation with xenon, the discharge voltage increased at discharge currents below 20 A, due to an insufficient self-heating of the emitter surface. With krypton, when the discharge current was increased above 20 A, the discharge voltage was found to increase as well, likely due to a less-efficient operation of the cathode at the higher current levels, in turn tied with the higher ionization energy of the propellant.

An example of electrical characteristic computed with the aid of the numerical code, for HC60 operated with the anode at 5 mg/s Xe, is shown in Fig. 12. The theoretical results can be compared with the measured anode voltages of about 16.5 V, for a current sweep from 30 to 50 A, even though the model of the plasma downstream of the keeper was not coupled with the cathode model yet. As a consequence, the theoretical values do not include any potential drop downstream of the keeper orifice. Figure 13 shows the cathode during the operation with keeper and anode (a), and during the coupling test with HT20k (b). In total, HC60 was operated for more than 300 hours, performing more than 130 ignitions.

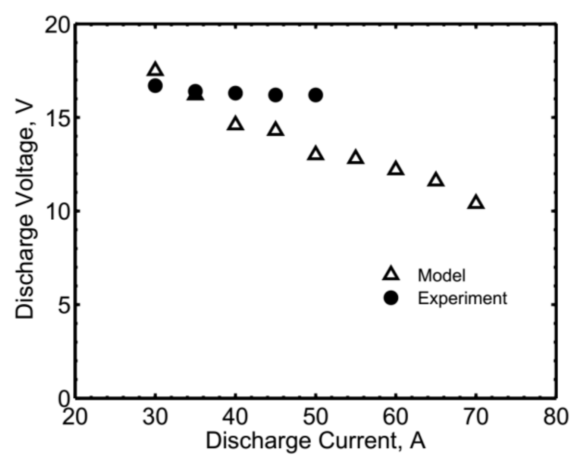

Figure 12. Comparison of experimental and theoretical electrical characteristics with floating keeper, at 5 mg/s Xe.

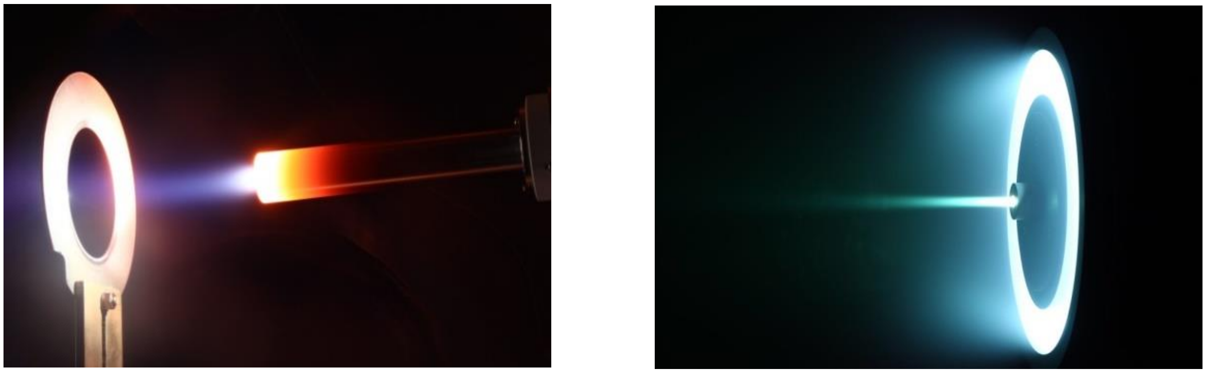

a) **b)**

Figure 13. a) HC60 in triode mode with 10 A keeper current and 38 A anode current. b) HC60 coupled with the Sitael HT20k[8].

VII. Conclusion

Hollow cathodes for 5 kW- and 20 kW- class Hall effect thrusters have been developed at Sitael, for current ranges of 8 – 20 A and 30 – 60 A, respectively. The cathodes were tested in stand-alone configuration, with both xenon and krypton propellants, and coupled with the thrusters. The results are promising and in good accordance with both experimental data available in the literature and the theoretical predictions coming from the model developed in-house. Future activities will include an improvement of the mechanical design of the cathodes, additional coupling tests with the thrusters, long-duration campaigns, as well as activities regarding the plasma diagnostics in the cathode plume. The latter experiments will allow for validating the results obtained from a model of the cathode plasma plume, to assess the model accuracy. Future developments of the theoretical activities will include the integration of the cathode model previously developed at Sitael with the plasma plume model, as well as a possible evolution to a 2D fluid model. A more extensive comparison between theoretical and experimental data will be also carried out to further validate the numerical results.

Acknowledgments

The authors wish to express their sincere gratitude to Cosimo Ducci, Federico Cannelli, Carlo Tellini, and Ugo Cesari for the testing activities, and to Giulia Becatti for post-processing the experimental data.

References

[1]Polk, J., Kakuda, R., Anderson, J., Brophy, J., Rawlin, V., Patterson, M., Sovey, J., and Hamley, J., "Validation of the NSTAR Ion Propulsion System on the Deep Space One Mission - Overview and Initial Results," AIAA99-2274, 35th AIAA/ASME/SAE/ASEE Joint Propulsion Conference and Exhibit, Los Angeles, CA, 1999.

[2]Racca, G., "SMART-1 from Conception to Moon Impact," Journal of Propulsion and Power, Vol. 25, No. 5, 2009, pp. 993–1002.

[3]Kuninaka, H., Nishiyama, K., Shimizu, Y., Hosoda, S., Koizumi, H., and Kawaguchi, J., "Status of Microwave Discharge Ion Engines on Hayabusa Spacecraft," AIAA 2007-5196, 43rd AIAA/ASME/SAE/ASEE Joint Propulsion Conference and Exhibit, Cincinnati, OH, 2007.

[4]Rayman, M. D., Fraschetti, T. C., Raymond, C. A., and Russell, C. T., "Dawn: A Mission in Development for Exploration of Main Belt Asteroids Vesta and Ceres," *Acta Astronautica*, Vol. 58, No. 11, 2006, pp. 605-616.

[5]Pedrini, D., Cannelli, F., Ducci, C., Misuri, T., Paganucci, F., and Andrenucci, M., "Hollow Cathodes Development at Sitael," SP2016_3124925, Space Propulsion Conference, Rome, Italy, 2 – 6 May 2016.

[6]Ducci, C., Andreussi, T., Arkhipov, A., Passaro, A., Andrenucci, M., Bulit, A., and Edwards, C., "Investigation of a 5 kW Class Hall-Effect Thruster Operating with Different Xenon-Krypton Mixtures," IEPC-2015-126/ISTS-2015-b-126, Joint Conference of 30th International Symposium on Space Technology and Science, 34th International Electric Propulsion Conference and 6th Nano-satellite Symposium, Hyogo-Kobe, Japan, 4 – 10 July 2015.

[7]Giannetti, V., Piragino, A., Faraji, F., Reza, M., Leporini, A., Saravia, M., Andreussi, T., Rossodivita, A., and Andrenucci, M., "Development of a 5 kW Low-Erosion Hall Effect Thruster," IEPC-2017-379, 35th International Electric Propulsion Conference Georgia Institute of Technology, Atlanta, GA, 8 – 12 October 2017.

[8]Piragino, A., Leporini, A., Giannetti, V., Pedrini, D., Rossodivita, A., Andreussi, T., Andrenucci, M., and Estublier, D., "Characterization of a 20 kW-Class Hall Effect Thruster," IEPC-2017-381, 35th International Electric Propulsion Conference Georgia Institute of Technology, Atlanta, GA, 8 – 12 October 2017.

[9]Misuri, T., Pergola, P., and Andrenucci, M., "HT5k Hall Thruster to Improve Small Launcher Capabilities," IEPC-2013-279, 33rd International Electric Propulsion Conference, Washington, DC, 6 – 10 October 2013.

[10]Lafferty, J. M., "Boride cathodes," *Journal of Applied Physics*, Vol. 22, No. 3, 1951, pp. 299–309.

[11]Yamauchi, H., Takagi, K., Yuito, I., and Kawabe, U., "Work function of LaB_6," *Applied Physics* Letters, Vol. 29, No. 10, 1976, pp. 638–640.

[12]Goebel, D. M., and Katz, I., *Fundamentals of Electric Propulsion: Ion and Hall Thrusters*, John Wiley and Sons, NJ, 2008.

[13]Albertoni, R., Pedrini, D., Paganucci, F., and Andrenucci, M., "A Reduced-Order Model for Thermionic Hollow Cathodes," *IEEE Transactions on Plasma Science*, Vol. 41, No. 7, June 2013, pp. 1731-1745.

[14]Pedrini, D., Albertoni, R., Paganucci, F., and Andrenucci, M., "Theoretical Model of a Lanthanum Hexaboride Hollow Cathode," *IEEE Transactions on Plasma Science*, Vol. 43, No. 1, November 2014, pp. 209-217.

[15]Domonkos, M. T., "Evaluation of Low-Current Orificed Hollow Cathodes," Ph.D. dissertation, Aerospace Engineering Dept., University of Michigan, Ann Arbor, MI, 1999.

[16]Downey, R. T. "Theoretical and Experimental Investigation into High Current Hollow Cathode Arc Attachment," Ph.D. dissertation, University of Southern California, CA, 2008.

[17]Mikellides, I. G., Katz, I., Goebel, D. M., and Jameson, K. K., "Evidence of Nonclassical Plasma Transport in Hollow Cathodes for Electric Propulsion," *Journal of Applied Physics*, Vol. 101, No. 6, pp. 063301-1–063301-11.

[18]Grassi, J., and Torrini, F., "Plasma Plume Modelling of Hollow Cathodes for Space Electric Thrusters," Master of Science Thesis in Aerospace Engineering and in Physics, University of Pisa, Pisa, Italy, 2017.

[19]Goebel, D. M., Jameson, K. K., Watkins, R. M., and Katz, I, "Hollow cathode and keeper-region plasma measurements using ultra-fast miniature scanning probes", 40th AIAA/ASME/SAE/ASEE Joint Propulsion Conference and Exhibit, Joint Propulsion Conferences, Fort Lauderdale, FL, 2004.

[20]Jameson, K. K., Goebel, D. M., and Watkins, R. M., "Hollow Cathode and Thruster Discharge Chamber Plasma Measurements," 29th IEPC International Electric Propulsion Conference, Princeton University, Princeton, NJ, 31 October – 4 November 2005.

[21]Potrivitu, G., "Low–voltage External Discharge Plasma Thruster and Hollow Cathodes Plasma Plume Diagnostics Utilising Electrostatic Probes and Retarding Potential Analyser", Master of Science Thesis in Space Technology, Department of Computer Science, Electrical and Space Engineering, Lulea University of Technology, 2016.

[22]Vranjes, J., and Kono, M., "Ion Plasma Wave and its Instability in Interpenetrating Plasmas," *Physics of Plasmas*, Vol. 21, No. 4, 2014, pp 042–104.

[23]Pedrini, D., Albertoni, R., Paganucci, F., and Andrenucci, M., "Development of a LaB_6 Cathode for High-Power Hall Thrusters," IEPC-2015-47/ISTS-2015-b-47, Joint Conference of 30th International Symposium on Space Technology and Science, 34th International Electric Propulsion Conference and 6th Nano-satellite Symposium, Hyogo-Kobe, Japan, 4 – 10 July 2015.

[24]Brophy, J. R., Brinza, D. E., Polk, J. E., and Henry, M. D., "The DS1 Hyper-Extended Mission," AIAA-2002-3673, 38th Joint Propulsion Conference, Indianapolis, IN, 2002.